Direct observation of exchange anisotropy in the helimagnetic insulator Cu_2OSeO_3

Priya R. Baral [1,2,3,*] Oleg I. Utesov [4] Chen Luo [5] Florin Radu [5] Arnaud Magrez [1]
Jonathan S. White [3] and Victor Ukleev [5,6,†]

[1]*Crystal Growth Facility, Institute of Physics, École Polytechnique Fédérale de Lausanne (EPFL), CH-1015 Lausanne, Switzerland*
[2]*Chair of Computational Condensed Matter Physics, Institute of Physics, École Polytechnique Fédérale de Lausanne (EPFL), CH-1015 Lausanne, Switzerland*
[3]*Laboratory for Neutron Scattering and Imaging (LNS), Paul Scherrer Institute (PSI), CH-5232 Villigen, Switzerland*
[4]*Center for Theoretical Physics of Complex Systems, Institute for Basic Science, Daejeon 34126, Republic of Korea*
[5]*Helmholtz-Zentrum Berlin für Materialien und Energie, D-14109 Berlin, Germany*
[6]*Swiss Light Source, Paul Scherrer Institute (PSI), CH-5232 Villigen, Switzerland*

The helical magnetic structures of cubic chiral systems are well explained by the competition among Heisenberg exchange, Dzyaloshinskii-Moriya interaction, cubic anisotropy, and anisotropic exchange interaction (AEI). Recently, the role of the latter has been argued theoretically to be crucial for the low-temperature phase diagram of the cubic chiral magnet Cu_2OSeO_3, which features tilted conical and disordered skyrmion states for a specific orientation of the applied magnetic field ($\mu_0\vec{H} \parallel [001]$). In this study, we exploit transmission resonant x-ray scattering in vector magnetic fields to directly quantify the strength of the AEI in Cu_2OSeO_3 and measure its temperature dependence. We find that the AEI continuously increases below 50 K, resulting in a conical spiral pitch variation of 10% in the (001) plane. Our results contribute to establishing the interaction space that supports tilted cone and low-temperature skyrmion state formation, facilitating the goals for both a quantitative description and eventual design of the diverse spiral states existing amongst chiral magnets.

In recent years, skyrmions in magnetic materials have attracted significant interest due to their potential spintronic functionalities that promise a paradigm shift in magnetic random access memory, data storage technologies, energy saving, and unconventional computing [1–3]. Skyrmions are typically found in thin films with asymmetric interfaces [4] and bulk noncentrosymmetric crystals, such as chiral and polar helimagnets [5,6].

The ground-state helical magnetic structures of cubic chiral systems are well described by the Bak-Jensen model, which considers the interplay between Heisenberg exchange interaction, Dzyaloshinskii-Moriya interaction (DMI), anisotropic exchange interaction (AEI), and cubic anisotropy (CA) [7–9]. The orientation of the helix axis is determined by a subtle interplay among DMI, AEI, and CA. The AEI has been broadly neglected due to its weak impact on experimental observations. However, both cubic and exchange anisotropies play a crucial role in determining the propagation direction of the helix [9] and, ultimately, the orientation of any field-induced skyrmion lattice (SkL) in these materials [10–12].

*priya.baral@psi.ch
†victor.ukleev@helmholtz-berlin.de

Moreover, in centrosymmetric materials the competition between AEI and single-ion anisotropy can stabilize SkL even without DMI [13]. In cubic chiral magnets, the nontrivial temperature evolution of anisotropic interactions has been demonstrated in $B20$s [15,16], β-Mn alloys [17,18], and Zn-doped Cu_2OSeO_3 [19]. Often, the unambiguous experimental distinction between the effects of cubic and exchange anisotropies is challenging since they both affect macroscopic parameters, such as the transition fields between helical and conical states and conical and field-polarized states [9,20]. Even neutron scattering techniques that are sensitive to microscopic material parameters are often unable to discriminate these two interactions without an additional theoretical model. According to phenomenological models, a fixed sign of the cubic anisotropy constant $K_c > 0$, ground-state helical spirals in cubic chiral magnets propagate along [100] axes in the case of a positive AEI constant $F_{AEI} > 0$ (e.g., in $Fe_{0.85}Co_{0.15}Si$ [21]) and along [111] axes if $F_{AEI} < 0$ (e.g., in MnSi [16]).

Notable examples in earlier work where the role of the AEI shows up clearly include in FeGe, where the reorientation of the spiral propagation vector is from [100] to [111] due to a sign change of the AEI [15], and in Zn-doped Cu_2OSeO_3, where a sign change of the AEI is also argued, albeit with no reorientation of the helix due to the predominance of CA [19].

Here, we focus on pristine Cu_2OSeO_3, a magnetoelectric chiral magnet with $T_C = 58$ K [22,23] which, in addition to conventional helical, conical, and SkL phases, also features several exotic metastable states, such as square and elongated

SkL phases [24,25]. Recently, the competition between the cubic and exchange anisotropies was argued to be crucial for the manifestation of unusual yet thermodynamically stable magnetic phases in Cu_2OSeO_3: tilted conical spiral and disordered skyrmions that emerge at low temperatures when a magnetic field is applied along one of the cubic axes [26–28]. Due to the magnetoelectric coupling of Cu_2OSeO_3 [23], its versatile magnetic phase diagram, and the ability to train the low-temperature skyrmion phase [25], the material is particularly interesting for exploring chiral magnet based applications paradigms [29]. Furthermore, developing the understanding of the fundamental mechanism of skyrmion stabilization through anisotropy engineering paves the way for magnetic phase manipulation amongst the known skyrmion hosts, which can be particularly relevant for room-temperature topological magnetic textures among noncentrosymmetric materials with high magnetic ordering temperatures such as chiral β-Mn-type alloys (T_C up to 400 K) [18] and $LiFe_5O_8$ (T_C ~900 K) [30]. Therefore, the unambiguous microscopic, quantitative determination of anisotropic interactions such as the AEI in model chiral magnets such as pristine Cu_2OSeO_3 is highly desirable.

Here we exploit the high momentum-space resolution of transmission resonant elastic x-ray scattering (t-REXS) in vector magnetic fields [31] to quantify directly the AEI in Cu_2OSeO_3. We obtain the following key results. First, the angular variation of the conical spiral pitch in the (100) plane observed by t-REXS agrees with a theory allowing the quantitative extraction of the AEI. Second, in contrast to both FeGe [15] and lightly Zn-doped Cu_2OSeO_3 [19], the sign of the AEI always remains negative across the entire temperature range below T_C. Third, the magnitude of the AEI increases continuously below 50 K, correlating with the stability window of the tilted cone and disordered skyrmion phases. Taken together, our results implicate the thermal evolution of the AEI and its competition with CA as determining the structure of the phase diagram and contribute quantitatively towards the foundation of the theoretical modeling and manipulation of spin textures in Cu_2OSeO_3 and other anisotropic chiral magnets.

In the isotropic case, the spiral propagation vector is proportional to the ratio of the DMI and exchange, $Q_0 \sim D/J$. When the anisotropic interactions come into play, the conical structure becomes distorted and, in general, contains an infinite number of harmonics and the exact solution for the spin structure can hardly be found. However, if the characteristic helical energy is much larger than the anisotropic contributions one can use a perturbative approach. In our case, in order to obtain corrections to the spiral vector, we obtain an approximate solution for the sine-Gordon equation describing an in-plane magnetization component with the anisotropy-induced terms. The latter are due to AEI, CA, and easy-plane anisotropy originating from the tensile strain of the lamella. Importantly, the leading order approximation allows us not to take into account small local variations of the conical angle. Details of the derivation of the following equation are given in the Supplemental Material [32].

At high temperatures the cubic anisotropy is small [33] (it is of the fourth order in the magnetization modulus) and we consider only the effect of AEI and easy plane. The result for

the spiral vector reads

$$Q = Q_0 \left\{ 1 - \frac{F_{AEI} \sin^2 2\psi}{4J} \right\} - \frac{JZ^2 \cot^2 \alpha}{2D^3} \sin^2 2(\psi - \phi)$$
$$- \frac{JZ^2}{8D^3} \sin^4(\psi - \phi). \tag{1}$$

Here ψ is the azimuth angle of the conical helicoid propagation vector in the (001) plane, α is the conical angle ($\alpha = 0$ in the fully polarized phase), Z is the easy-plane anisotropy constant, and ϕ indicates the corresponding axis direction. At small temperatures the AEI-induced correction in the first term of Eq. (1) dominates, with other terms, including the one stemming from CA (see [32]), being less prominent. In addition, we have tried to fit the experimental data considering the higher-order exchange anisotropy term and found that the result is the same within the error bar. Therefore, it is excluded from the analysis.

A polar plot of the spiral wave vector Q depending on its orientation in the (001) is shown in Fig. 1(a) for positive and negative F_{AEI} constants as an example. For $F_{AEI} > 0$, the propagation vector of the spiral in the ground state is favored by AEI along $\langle 001 \rangle$, while for negative F_{AEI} spirals propagate along diagonals of the cubic lattice $\langle 111 \rangle$. Experimentally, the conical propagation vector can be determined at will azimuthally in the (001) crystal plane by a finite vector magnetic field [Fig. 1(b)]. The detailed description of the samples and the measurement setup is given in the Supplemental Material [32]. Each conical state was prepared using the following procedure. First, the helical state was achieved by cooling the sample down to the target temperature at zero field ($T = 14$ K), followed by ramping up the magnetic field to 70 mT to force the sample into the field-polarized state. The field was then ramped down to 30 mT in order to remain inside the conical phase for a particular ψ. After each acquisition, the magnetic field was again ramped up to 70 mT, followed by changing its in-plane direction. This protocol was repeated for each ψ ranging between 0 and 180° with a 3° step.

At each particular sample temperature, the intensity corresponding to each of the Friedel pair of conical peaks for the measured ψ was extracted and summed up. The resulting patterns measured at the lowest (14 K), intermediate (25 K), and highest (50 K) temperatures are shown in Figs. 1(d)–1(f). At $T = 50$ K, the intensity profile appears almost circular, but with a slight elliptical distortion [1(f)]. The observed ellipticity in the intensity profile is an indication of the uniaxial anisotropy induced by strain arising from the contacts made on the lamella sample during FIB milling [34–36]. As the temperature decreases, the profile starts to develop subtle features along the marked crystallographic axes. On cooling, the azimuthal scattering intensity distribution profile deviates from the ellipticity seen at 50 K and develops extra humps along the in-plane [110] directions. This is most strongly pronounced at the base temperature of 14 K, as shown in [1(d)]. Concomitantly, $|Q|$ along the [100] directions is found to be the minimum and $Q||[110]$ the maximum. Interestingly, in contrast to FeGe [31], the helical spiral was observed to always revert the orientation of propagation back to the [100] direction upon leaving the in-plane conical phase through
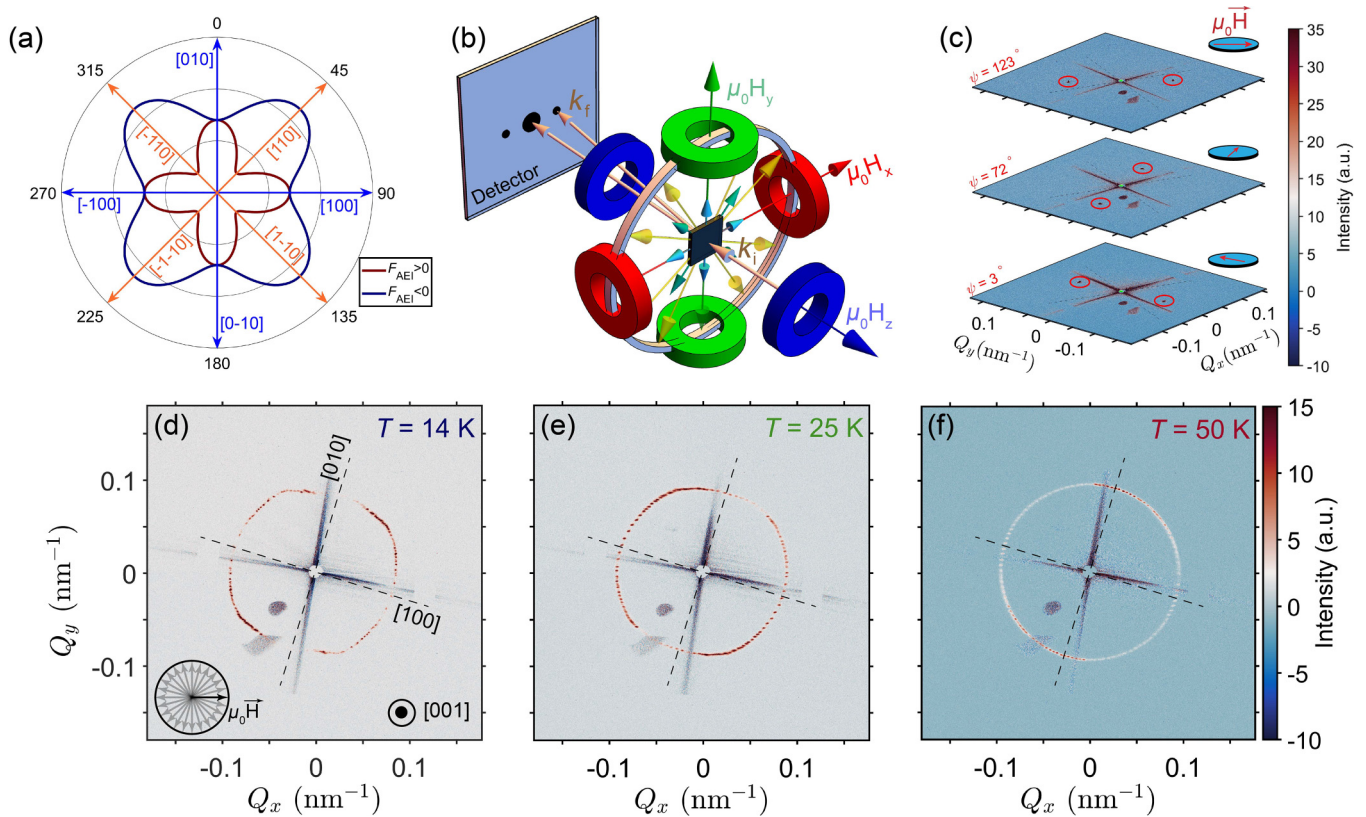
FIG. 1. (a) Illustration of the spiral modulation vector Q dependence on azimuthal angle in (110) plane for positive and negative signs of the exchange anisotropy constant, F_{AEI}. (b) Sketch of the geometry of the t-REXS experiment at VEKMAG [14]. The magnetic field was vectorially varied in the x-y plane. (c) t-REXS patterns measured in conical states for different azimuthal angles, $\psi = 3°, 72°, 123°$ at $T = 14$ K. Sum of the t-REXS patterns over all measured ψ angles from 0 to 180° at (d) 14 K, (e) 25 K, and (f) 50 K.

reduction of the field. This is another manifestation of the strong CA in Cu_2OSeO_3.

In the next step, both the radial and azimuthal profiles of the diffracted intensity at each ψ were examined. In order to only contain a single Bragg peak, a sector box of 3° angular width was chosen around each. Also, both peaks from the Friedel pair were analyzed separately, using mirror sectors, providing us with information on $|Q|$ in all four quadrants simultaneously. Polar plots of the extracted peak position $Q_c(\psi)$ in Figs. 2(a)–2(f) directly show the anisotropic nature of the conical spirals in Cu_2OSeO_3 and how this develops on cooling. The direct influence of temperature dependence of the AEI on $|Q_c|$ can be seen clearly in Fig. 2. At the lowest $T = 14$ K [Fig. 2(a)], Q_c varies from 0.086 nm^{-1} along [100] to 0.092 nm^{-1} along [110] in a monotonous fashion, as it is expected according to Eq. (1). This shows that in Cu_2OSeO_3 the AEI is most pronounced at low temperatures, resulting in the conical spiral pitch variation up to 10% between the conical spirals oriented along [100] and [110].

In order to quantify the AEI constant, $Q(\psi)$ dependencies were fitted according to Eq. (1) (solid lines in Fig. 2). The result is shown in Fig. 3, where $|F_{AEI}|$ clearly tends to monotonically increase towards low temperatures, reaches $F_{AEI} = -0.163 \pm 0.012$ pJm^{-1} at 14 K, and practically vanishes at 50 K. The strain-induced anisotropy terms containing Z in Eq. (1) do not show significant variation as a function of temperature (see the Supplemental Material [32]).

The sign of the AEI constant F_{AEI} in Cu_2OSeO_3 is negative in the whole temperature range, in contrast to previous results on Zn-doped Cu_2OSeO_3 (Fig. 3) [19]. As shown before, a few percent Zn doping can modify the microscopic properties of pristine Cu_2OSeO_3 significantly [37] and our data supports this conclusion. Moreover, this suggests that one can tune the microscopic parameter with a small doping and hence finely tailor the helical (skyrmion lattice) pitch and stability windows of anisotropy-driven phases. Importantly, at low temperatures the two systems consistently demonstrate the strong contribution of the magnetocrystalline anisotropy that pins the spiral wave vector along [100]. Nonetheless, the competition between the AEI and cubic anisotropies favoring different orientation of magnetic spirals is known to stabilize more unusual magnetic spiral superstructures such as tilted conical and disordered skyrmion phases [10,26,28]. A fine balance between AEI and CA is required to theoretically reproduce low-temperature magnetic phases in Cu_2OSeO_3 [28]. The strong enhancement of the AEI at low temperatures is evident from our data and provides a much needed quantitative basis for the stability of tilted conical and disordered skyrmion states proposed by the theory. Therefore, a chemical tuning of the AEI would be a promising approach to stabilize new phases far below T_C in other known cubic chiral magnets.

In summary, the study of the anisotropic exchange interaction (AEI) in the cubic chiral magnet Cu_2OSeO_3 using
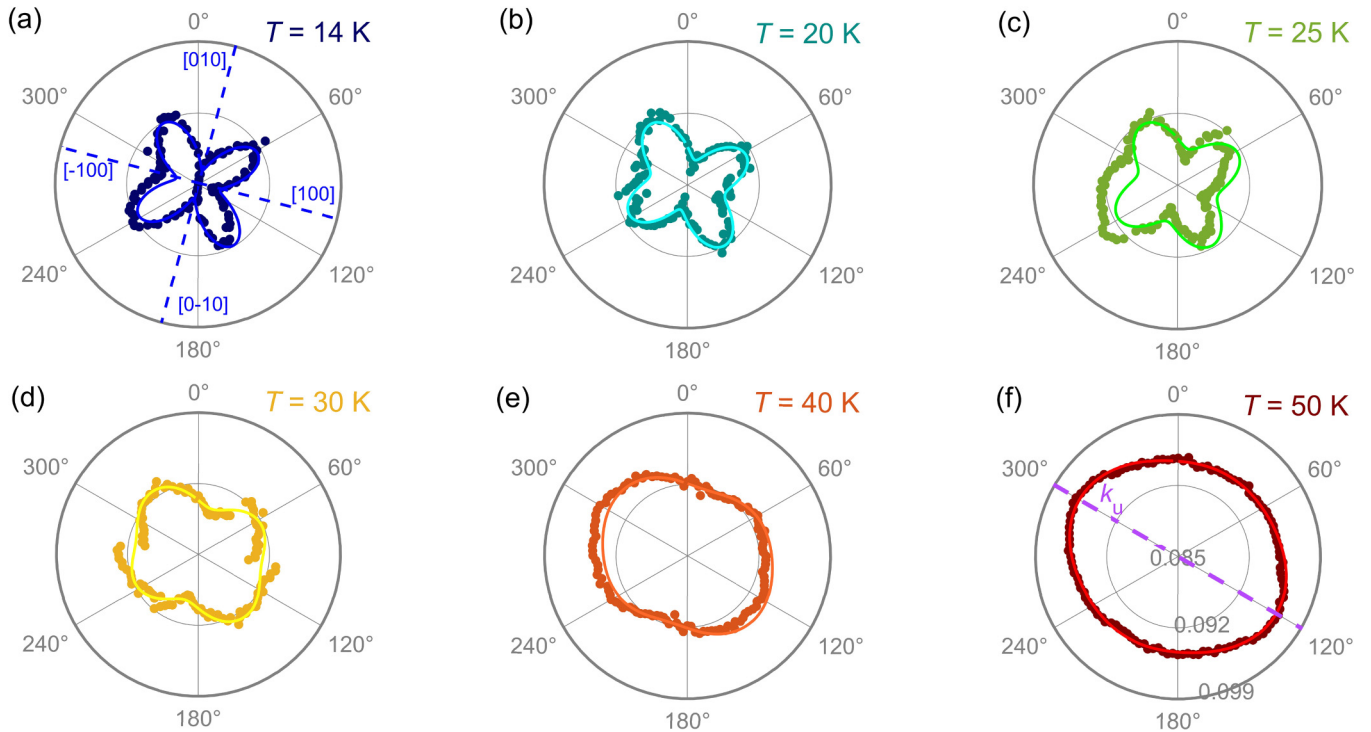
FIG. 2. Polar plots of the extracted conical spiral wave vector Q as a function of angle ψ at (a) 14 K, (b) 20 K, (c) 25 K, (d) 30 K, (e) 40 K, and (f) 50 K. Solid lines correspond to the fit according to Eq. (1) including the offset of 17° between $\psi = 0°$ and [100] axis due to imperfect sample mounting (see the Supplemental Material for more details on the sample orientation [32]). The radial scale for Q is given in panel (f) and is the same for all panels (a)–(f).

transmission resonant x-ray scattering in vector magnetic fields has revealed that the sign of the AEI energy constant is negative in the whole temperature range below T_C, and continuously increases below 50 K, to reach $F_{AEI} = -0.163$ pJm^{-1} at our lowest temperature of 14 K. The sign of the AEI constant is negative in the whole temperature range, pointing to a stronger contribution of cubic anisotropy that pins the

FIG. 3. Temperature dependence of the exchange anisotropy constant F_{AEI} extracted from the fit of $Q(\psi)$ according to Eq. (1). The black dashed line is a guide to the eye.

spiral propagation vector along [001]. The magnitude of F_{AEI} is of the same order as in FeGe but with an opposite sign. Our measurements of the strong enhancement of the AEI at low temperatures provide a quantitative basis for phenomenological theories that describe how competing anisotropies in chiral magnets can stabilize novel complex spiral magnetic states such as tilted conical and disordered skyrmion phases. Additionally, we have presented a theoretical and experimental framework for quantifying AEI in cubic chiral magnets and distinguishing it from CA, which is valuable for comparison with *ab initio* theories and for understanding the role of AEI in the emergence of skyrmions and other exotic magnetic states. A similar approach can be further developed for a broader class of anisotropic magnets with long-periodic spin modulations stabilized by other mechanisms, such as frustrated interactions [38–40].
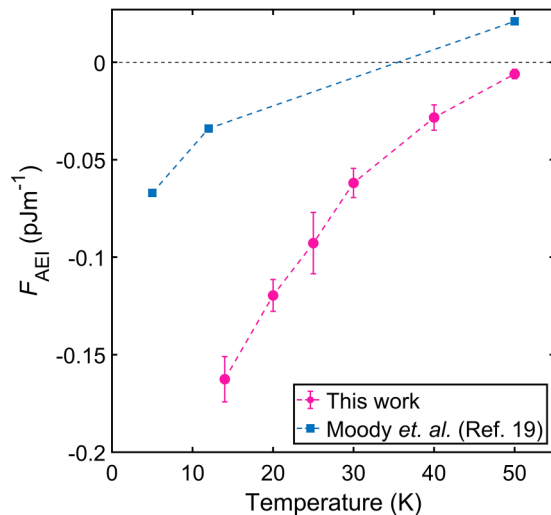
[1] A. Fert, N. Reyren, and V. Cros, Magnetic skyrmions: Advances in physics and potential applications, Nat. Rev. Mater. **2**, 17031 (2017).

[2] K. Everschor-Sitte, J. Masell, R. M. Reeve, and M. Kläui, Perspective: Magnetic skyrmions–overview of recent progress in an active research field, J. Appl. Phys. **124**, 240901 (2018).

[3] K. M. Song, J.-S. Jeong, B. Pan, X. Zhang, J. Xia, S. Cha, T.-E. Park, K. Kim, S. Finizio, J. Raabe *et al.*, Skyrmion-based artificial synapses for neuromorphic computing, Nat. Electron. **3**, 148 (2020).

[4] J. Sampaio, V. Cros, S. Rohart, A. Thiaville, and A. Fert, Nucleation, stability and current-induced motion of isolated magnetic skyrmions in nanostructures, Nat. Nanotechnol. **8**, 839 (2013).

[5] A. Bogdanov and A. Hubert, Thermodynamically stable magnetic vortex states in magnetic crystals, J. Magn. Magn. Mater. **138**, 255 (1994).

[6] Y. Tokura and N. Kanazawa, Magnetic skyrmion materials, Chem. Rev. **121**, 2857 (2021).

[7] P. Bak and M. H. Jensen, Theory of helical magnetic structures and phase transitions in MnSi and FeGe, J. Phys. C **13**, L881 (1980).

[8] O. Nakanishi, A. Yanase, A. Hasegawa, and M. Kataoka, The origin of the helical spin density wave in MnSi, Solid State Commun. **35**, 995 (1980).

[9] S.V. Maleyev, Cubic magnets with Dzyaloshinskii-Moriya interaction at low temperature, Phys. Rev. B **73**, 174402 (2006).

[10] A. O. Leonov, C. Pappas, and I. Kézsmárki, Field and anisotropy driven transformations of spin spirals in cubic skyrmion hosts, Phys. Rev. Res. **2**, 043386 (2020).

[11] T. Adams, M. Garst, A. Bauer, R. Georgii, and C. Pfleiderer, Response of the Skyrmion Lattice in MnSi to Cubic Magnetocrystalline Anisotropies, Phys. Rev. Lett. **121**, 187205 (2018).

[12] J. Kindervater, T. Adams, A. Bauer, F. X. Haslbeck, A. Chacon, S. Mühlbauer, F. Jonietz, A. Neubauer, U. Gasser, G. Nagy *et al.*, Evolution of magnetocrystalline anisotropies in $Mn_{1-x}Fe_xSi$ and $Mn_{1-x}Co_xSi$ as inferred from small-angle neutron scattering and bulk properties, Phys. Rev. B **101**, 104406 (2020).

[13] M. Hirschberger, S. Hayami, and Y. Tokura, Nanometric skyrmion lattice from anisotropic exchange interactions in a centrosymmetric host, New J. Phys. **23**, 023039 (2021).

[14] T. Noll and F. Radu, The mechanics of the VEKMAG experiment, *Proc. of MEDSI2016, Barcelona, Spain, 2016*, edited by Volker R. W. Schaa (JACoW, Geneva, Switzerland, 2017), pp. 370–373.

[15] B. Lebech, J. Bernhard, and T. Freltoft, Magnetic structures of cubic fege studied by small-angle neutron scattering, J. Phys.: Condens. Matter **1**, 6105 (1989).

[16] S. V. Grigoriev, D. Chernyshov, V. A. Dyadkin, V. Dmitriev, S. V. Maleyev, E. V. Moskvin, D. Menzel, J. Schoenes, and H. Eckerlebe, Crystal Handedness and Spin Helix Chirality in $Fe_{1-x}Co_xSi$, Phys. Rev. Lett. **102**, 037204 (2009).

[17] M. Preißinger, K. Karube, D. Ehlers, B. Szigeti, H.-A. Krug von Nidda, J. White, V. Ukleev, H. Rønnow, Y. Tokunaga, A. Kikkawa *et al.*, Vital role of magnetocrystalline anisotropy in cubic chiral skyrmion hosts, npj Quantum Mater. **6**, 1 (2021).

[18] K. Karube, J. S. White, V. Ukleev, C. D. Dewhurst, R. Cubitt, A. Kikkawa, Y. Tokunaga, H. M. Rønnow, Y. Tokura, and Y. Taguchi, Metastable skyrmion lattices governed by magnetic disorder and anisotropy in β-Mn-type chiral magnets, Phys. Rev. B **102**, 064408 (2020).

[19] S. H. Moody, P. Nielsen, M. N. Wilson, D. A. Venero, A. Štefančič, G. Balakrishnan, and P. D. Hatton, Experimental evidence of a change of exchange anisotropy sign with temperature in Zn-substituted Cu_2OSeO_3, Phys. Rev. Res. **3**, 043149 (2021).

[20] S. V. Grigoriev, A. S. Sukhanov, and S. V. Maleyev, From spiral to ferromagnetic structure in B20 compounds: Role of cubic anisotropy, Phys. Rev. B **91**, 224429 (2015).

[21] S. V. Grigoriev, S. V. Maleyev, A. I. Okorokov, Y. O. Chetverikov, P. Böni, R. Georgii, D. Lamago, H. Eckerlebe, and K. Pranzas, Magnetic structure of MnSi under an applied field probed by polarized small-angle neutron scattering, Phys. Rev. B **74**, 214414 (2006).

[22] S. Seki, X. Yu, S. Ishiwata, and Y. Tokura, Observation of skyrmions in a multiferroic material, Science **336**, 198 (2012).

[23] J. S. White, K. Prša, P. Huang, A. A. Omrani, I. Živković, M. Bartkowiak, H. Berger, A. Magrez, J. L. Gavilano, G. Nagy *et al.*, Electric-Field-Induced Skyrmion Distortion and Giant Lattice Rotation in the Magnetoelectric Insulator Cu_2OSeO_3, Phys. Rev. Lett. **113**, 107203 (2014).

[24] R. Takagi, Y. Yamasaki, T. Yokouchi, V. Ukleev, Y. Yokoyama, H. Nakao, T. Arima, Y. Tokura, and S. Seki, Particle-size dependent structural transformation of skyrmion lattice, Nat. Commun. **11**, 5685 (2020).

[25] A. Aqeel, J. Sahliger, T. Taniguchi, S. Mändl, D. Mettus, H. Berger, A. Bauer, M. Garst, C. Pfleiderer, and C. H. Back, Microwave Spectroscopy of the Low-Temperature Skyrmion State in Cu_2OSeO_3, Phys. Rev. Lett. **126**, 017202 (2021).

[26] F. Qian, L. J. Bannenberg, H. Wilhelm, G. Chaboussant, L. M. Debeer-Schmitt, M. P. Schmidt, A. Aqeel, T. T. Palstra, E. Brück, A. J. Lefering *et al.*, New magnetic phase of the chiral skyrmion material Cu_2OSeO_3, Sci. Adv. **4**, eaat7323 (2018).

[27] A. Chacon, L. Heinen, M. Halder, A. Bauer, W. Simeth, S. Mühlbauer, H. Berger, M. Garst, A. Rosch, and C. Pfleiderer, Observation of two independent skyrmion phases in a chiral magnetic material, Nat. Phys. **14**, 936 (2018).

[28] L. J. Bannenberg, H. Wilhelm, R. Cubitt, A. Labh, M. P. Schmidt, E. Lelièvre-Berna, C. Pappas, M. Mostovoy, and A. O. Leonov, Multiple low-temperature skyrmionic states in a bulk chiral magnet, npj Quantum Mater. **4**, 11 (2019).

[29] O. Lee, T. Wei, K. D. Stenning, J. C. Gartside, S. Seki, A. Aqeel, C. Back, Y. Tokura, W. R. Branford, and H. Kurebayashi, Task-adaptive physical reservoir computing, arXiv:2209.06962.

[30] Y. Iguchi, S. Uemura, K. Ueno, and Y. Onose, Nonreciprocal magnon propagation in a noncentrosymmetric ferromagnet LiFe$_5$O$_8$, Phys. Rev. B **92**, 184419 (2015).

[31] V. Ukleev, O. Utesov, L. Yu, C. Luo, K. Chen, F. Radu, Y. Yamasaki, N. Kanazawa, Y. Tokura, T.-h. Arima, and J. S. White, Signature of anisotropic exchange interaction revealed by vector-field control of the helical order in a FeGe thin plate, Phys. Rev. Res. **3**, 013094 (2021).

[32] See Supplemental Material at http://link.aps.org/supplemental/10.1103/PhysRevResearch.5.L032019 for details on the sample preparation, t-REXS experiment, temperature dependence of the Z parameter, and analytical derivation of the conical wave vector in the presence of anisotropic interactions.

[33] S. Grigoriev, N. Chubova, L. Azarova, and O. Utesov, Transition from spiral to ferromagnetic structure in Fe$_{1-x}$Co$_x$Si compounds: Small-angle neutron scattering study, Ann. Phys. (NY) **447**, 169132 (2022).

[34] K. Shibata, J. Iwasaki, N. Kanazawa, S. Aizawa, T. Tanigaki, M. Shirai, T. Nakajima, M. Kubota, M. Kawasaki, H. Park *et al.*, Large anisotropic deformation of skyrmions in strained crystal, Nat. Nanotechnol. **10**, 589 (2015).

[35] Y. Okamura, Y. Yamasaki, D. Morikawa, T. Honda, V. Ukleev, H. Nakao, Y. Murakami, K. Shibata, F. Kagawa, S. Seki *et al.*, Directional electric-field induced transformation from skyrmion lattice to distinct helices in multiferroic Cu$_2$OSeO$_3$, Phys. Rev. B **95**, 184411 (2017).

[36] V. Ukleev, Y. Yamasaki, O. Utesov, K. Shibata, N. Kanazawa, N. Jaouen, H. Nakao, Y. Tokura, and T.-h. Arima, Metastable solitonic states in the strained itinerant helimagnet FeGe, Phys. Rev. B **102**, 014416 (2020).

[37] A. Štefančič, S. H. Moody, T. J. Hicken, M. T. Birch, G. Balakrishnan, S. A. Barnett, M. Crisanti, J. S. O. Evans, S. J. R. Holt, K. J. A. Franke *et al.*, Origin of skyrmion lattice phase splitting in Zn-substituted Cu$_2$OSeO$_3$, Phys. Rev. Mater. **2**, 111402 (2018).

[38] R. Ballou, J. Deportes, R. Lemaire, Y. Nakamura, and B. Ouladdiaf, Helimagnetism in the cubic laves phase YMn$_2$, J. Magn. Magn. Mater. **70**, 129 (1987).

[39] X. Yu, M. Mostovoy, Y. Tokunaga, W. Zhang, K. Kimoto, Y. Matsui, Y. Kaneko, N. Nagaosa, and Y. Tokura, Magnetic stripes and skyrmions with helicity reversals, Proc. Natl. Acad. Sci. USA **109**, 8856 (2012).

[40] S.-Z. Lin and S. Hayami, Ginzburg-Landau theory for skyrmions in inversion-symmetric magnets with competing interactions, Phys. Rev. B **93**, 064430 (2016).